Modeling Particle Hydrodynamic Transport in an Idealized Nanoscale Bio-Motor

P. Worth Longest and Ramana Pidaparti

Department of Mechanical Engineering
Virginia Commonwealth University
Richmond, VA 23284
E-mail: pwlongest@vcu.edu or rmpidaparti@vcu.edu

ABSTRACT

The supra-molecular motor, called the nuclear pore complex (NPC), controls the transport of all cellular material between the cytoplasm and the nucleus that occurs naturally in all biological cells. It consists of a large number of spatially organized proteins that, together with soluble transport factors, manage to export, import and exclude proteins with remarkable speed and fidelity. The NPC operates primarily via energy dependent processes, and performs some of the most vital functions required for the survival of a cell. In the presence of appropriate chemical stimuli, the NPC opens or closes, like a gate, and permits the flow of material into and out of the nucleus. The objective of this study is to better understand the hydrodynamic and particle transport characteristics of the NPC in order to potentially apply this highly effective structure to other nanoscale applications. An idealized model of NPC containing the central plug, bottom basket and top cytoplasm rings similar to a model described in the literature will be considered.

Keywords: bio-motor, nuclear pore complex, bio-inspired design, CFD, FEA

1 INTRODUCTION

Molecular motors, pumps and sorters are nature's nanomachines. They are the essential agents of movement and integral parts of many living organisms. These multifunctional molecular structures are far more efficient than any man made actuators. The nuclear pore complex (NPC) is a multifunctional structure composed of many molecules, i.e., a supramolecular structure.

The nuclear pore complex (NPC) controls the transport of all cellular material between the cytoplasm and the nucleus that occurs in all biological cells. It consists of a large number of spatially organized proteins that, together with soluble transport factors, manage to export, import and exclude proteins with remarkable speed and fidelity. The NPC operates via hydrodynamic and energy dependent processes, and performs some of the most vital functions required for the survival of a cell. In the presence of appropriate chemical stimuli, the NPC opens or closes, like a gate, and permits and modulates the flow of material into and out of the nucleus. The NPC has typical dimensions of 100-200 nm, making it a megadalton (MDa) heteromultimeric protein complex, which spans the nuclear envelope and is postulated to possess a transporter-containing a central cylindrical body embedded between cytoplasmic and nucleoplasmic rings [1]. A cell has many, presumably identical, NPCs, each of which participates in the import and export of nuclear material from within the nucleus (see Fig. 1). Exactly how this transport through the NPC occurs is an open question, and an important one, with profound implications for the design of micro/nanoscale devices for fluidic transport, genetic engineering and targeted drug delivery.

An overview of the proposed approach to uncover the design characteristics and study transport dynamics and mechanical characteristics of the bio-inspired NPC is shown in Fig. 1. The proposed approach of using a combination of mathematical and computational modeling methodologies along with scaled prototype models offers a unique and novel way to uncover the critical design criteria in terms of efficiency (power conversion), speed, and robustness for the bio-inspired supramolecular structure. The identified design criteria at a nano-level will help in developing a best design for a specific application. The developed criteria can be integrated with decision tools in a seamless fashion to design multi-functional macro/micro/nanoscale devices.

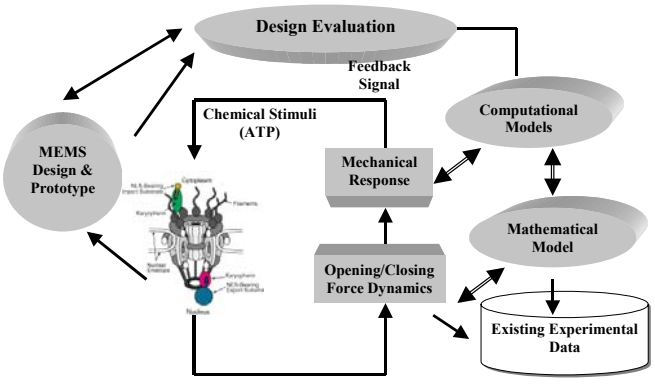

Fig. 1: Overview of bio-inspired design evaluation

2 METHODS

Computational fluid dynamics (CFD) and finite element structural analyses of the NPC have been initialized. An idealized model of the NPC structure has been considered which contains key elements for hydrodynamic and dispersed particle transport. Specifically, the simplified NPC-based structure consists of an hour-glass shaped base, the bottom basket, and the central element, as shown in Fig 2.

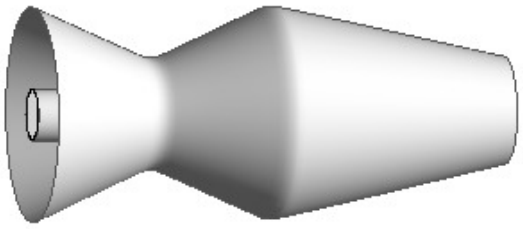

Fig. 2: Simplified surface model of NPC-based structure

2.1 Structural Analysis

ANSYS software was used to perform a structural finite element analysis. The finite element model consists of various elements (shell, membrane, solid, and beam) and fluid element based viscous/non-viscous media. Convergence studies were conducted to estimate the level of mesh refinement required for 1% accuracy of results.

Each of the structural elements are treated as a linear elastic material. Material properties for the structural elements are not known but some studies suggest that it is more like a cell material, hence the properties of the cell will be used from the existing experimental data [2].

The results of deformations/stresses are obtained from the structural analysis. Future parametric studies will be conducted to see the range of results when the structural/material properties are varied. A sensitivity study will also be carried out to see how the perturbations in design features change the results in terms of mechanical efficiency of the structure.

2.2 CFD Analysis

Computational evaluation of the NPC-based pumping structure requires solving the governing conservation equations for mass, momentum and dilute chemical species on a moving mesh, as shown below for incompressible laminar flow [3]:

$$\frac{\rho g}{\sqrt{g}}\frac{\partial}{\partial t}\left(\sqrt{g}\right)+\rho g\frac{\partial}{\partial x_j}\left(u_j-\frac{\partial \tilde{x}_j}{\partial t}\right)=0 \qquad (1)$$

$$\frac{\rho g}{\sqrt{g}}\frac{\partial}{\partial t}\left(\sqrt{g}\,u_i\right)+\rho g\frac{\partial}{\partial x_j}\left[\left(u_j-\frac{\partial \tilde{x}_j}{\partial t}\right)u_i\right]=-\frac{\partial p}{\partial x_i}+\mu\frac{\partial^2 u_i}{\partial {x_j}^2} \qquad (2)$$

$$\frac{\rho g}{\sqrt{g}}\frac{\partial}{\partial t}\left(\sqrt{g}\,\omega_S\right)+\rho g\frac{\partial}{\partial x_j}\left[\left(u_j-\frac{\partial \tilde{x}_j}{\partial t}\right)\omega_S\right]=\rho g\,D_S\frac{\partial^2 \omega_S}{\partial {x_j}^2} \qquad (3)$$

In these equations, $\tilde{x}_i$ represents the moving mesh location and $\sqrt{g}$ is the metric tensor determinate of the transformation, i.e., the local computational control-volume size. The above equations are for continuum flow. For liquid flow in a 100 nm structure, noncontinuum effects will become significant and must be accounted for using correction models. For liquid flow, the no-slip boundary condition will be assumed valid at the wall [4]. However, electrostatic, surface tension, and surface roughness effects may be significant. Electrostatic forces and surface tension can be modeled directly [4, 5]. To address surface roughness, near-wall porous media and roughness viscosity models will be employed [6, 7].

2.3 Discrete Element Transport

Evaluation of the sorting characteristics of the simplified NPC-based structure shown in Fig. 1 requires tracking discrete elements and predicting their interaction with the inner and outer walls. For sufficiently small discrete elements and perfect wall absorption, the continuum equation for dilute chemical species may be used. However, this methodology is not capable of predicting the wall and fluid interactions of the 5 nm – 20 nm discrete elements of interest here. Alternately, a model based on Newton's Second Law that can be used to approximate particle wall interactions and can be expressed as [8]

$$\frac{dv_i}{dt}=\frac{f_d}{\tau_p C_c}\left(u_i-v_i\right)+f_{i,\text{near-wall}}+f_{i,brown}+f_{i,turb}+f_{i,electrostatic}$$

$$\frac{dx_i}{dt}=v_i(t) \qquad (4a \& b)$$

In the above equations, v_i and u_i are the components of the particle and local fluid velocity, respectively. The characteristic time required for particles to respond to changes in the flow field, or the momentum response time, is $\tau_p = \rho_p d_p^2/18\eta$. The first term on the right hand side of Eq. (4a) represents particle drag including the Cunningham correction factor for molecular slip. The drag coefficient f_d for rigid and deformable particles is available from Clift et al. [9]. Brownian motion, which arises from molecular collisional effects on small particles and results in diffusion, is represented as a stochastically fluctuating force with zero mean and a 3-D variance of $6Dt$ where D is this diffusion

coefficient available from the Stokes-Einstein equation [10]. Calculation of the near-wall forces has been described in Longest et al. [8].

To solve the equations governing fluid flow and discrete element transport, a commercial CFD package (FLUENT) was used. In order to resolve the extremely small scales of interest, non-dimensional scaling of the system was implemented, along with double precision calculations. User defined routines were employed to model nanoscale transport phenomena and non-continuum effects not accounted for in this general purpose code.

3 RESULTS

3.1 Structural Analysis

As a first step in understanding the mechanical characteristics of the NPC, a preliminary study was conducted to understand the force-deformation characteristics of the simplified NPC-based model. The central plug is connected to the bottom basket through the filaments and at the top with the cytoplasmic ring and filaments. The model is constrained at the nuclear envelope. The NPC structure was modeled using shell elements for the outer surface (SHELL63), a three-dimensional solid for the central plug (SOLID92), and the basket and cytoplasmic filaments modeled as beam elements (BEAM3) in the ANSYS finite element software. Each structural element is nanometric in size, representing various components of the NPC structure.

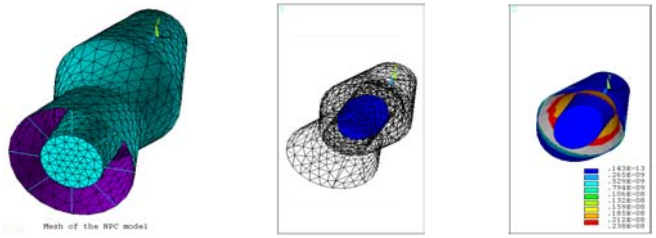

Fig. 3: Idealized bio-inspired model, deformation, stresses and velocity contours from analysis

Figure 3 shows the deformation and stress distribution in the NPC at a medium range of force applied to the central plug. The solid central plug deformation is about 5 times when the force is varied from low to high. Similarly, the local stresses at the interface between central plug and the nuclear envelope is about 3-4 times when the force is varied from low to high. The finite element analysis will be able to determine the local distribution of stress and strain, which can be used to characterize the local deformation phenomena of the NPC.

3.2 CFD Analysis

The hexahedral computational grid used to discretized the flow field equations is shown in Fig. 4. Velocity magnitude at the midplane and selected cross-sectional locations is shown in Fig. 5 for a uniform input velocity of 0.6 cm/s.

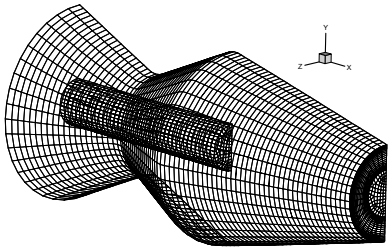

Fig. 4: Hexahedral computational grid.

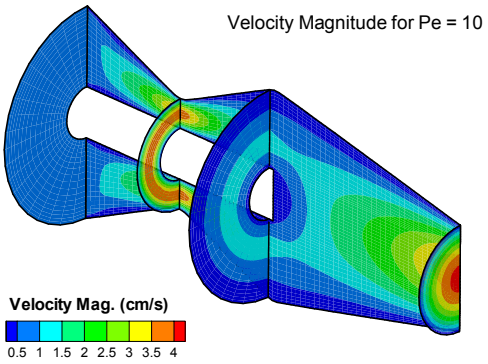

Fig. 5: Velocity magnitude for a uniform velocity inlet of 0.6 cm/s

As a case study, 10 nm particles were initialized uniformly over the inlet and tracked under steady flow conditions (Fig. 6). A Peclet number to describe the discrete phase can be defined as Pe = VL/D where V and L represent the characteristic velocity and diameter of the simplified NPC-based structure, and D is the diffusion coefficient of the discrete elements. As such, the Peclet number represents the ratio of convective fluid motion to particle diffusion. Particles have been assumed to be spherical and non-hydrated, and the Stokes-Einstein relation has been used to estimate particle diffusivity.

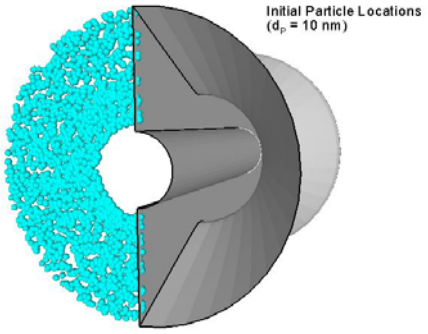

Fig. 6: Uniform particle initialization plane

Simulations of particle trajectories for PE = 1 (diffusion dominant flow) indicate that random particle motions result in wall contacts for all particles in the upstream region of the geometry (Fig. 7a). As convective forces are increased (Pe = 100) random motions remain largely evident along the particle tracts. However, some particles are able to escape the geometry without contacting the wall surface (Fig. 7b). For convection dominated flows (Pe = 10,000) a much smaller fraction of particles contacts the NPC wall.

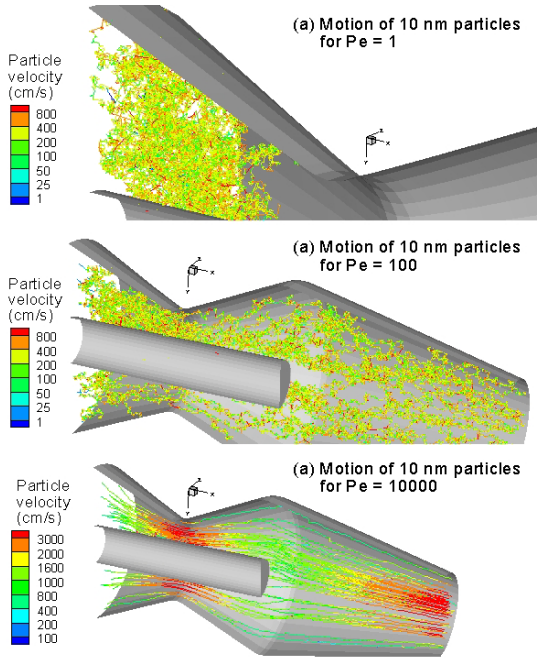

Fig. 7: Particle trajectories through the NPC for (a) Pe = 1; (b) Pe = 100; (c) Pe = 10,000.

Deposition locations shown in Figure 8 indicate that particles with lower Peclet numbers rapidly deposit on the upstream portion of the NPC-based structure. As the Peclet number is increased, deposition fractions are reduced and deposition locations are shifted downstream. Deposition fractions for a range of Pe values (0.1 – 10,000) demonstrate an effective cutoff value, beyond which the deposition function is significantly reduced.

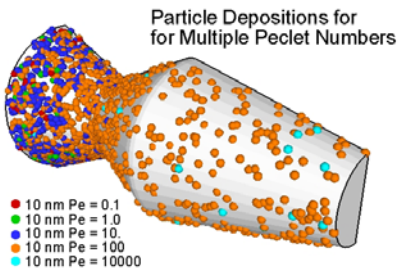

Fig. 8: Internal particle deposition locations for 10 nm particles at various Peclet numbers.

4 DISCUSSION

Our future investigation of bio-inspired supramolecular nanomachine design and simulation will involve a multidisciplinary, collaborative approach consisting of theoretical and computational models involving multiphase transport, elastodynamics, and coupled fluid-structure interactions, as well as engineering design, fabrication, and optimization. Specifically, we will investigate the characteristics of the biological structure through design analysis and simulations and develop a scaled prototype to evaluate the issues related to performance, applications and manufacturability of various components.

REFERENCES

1. Akey, C.W. and M. Radmacher, *Architecture of the Xenopus Nuclear Pore Complex revealed by three-dimensional cryo-electron microscopy.* J. Cell Biol., 1993. **122**: p. 1-19.
2. Kiseleva, E., et al., *Active nuclear pore complexes in Chironomus: visualization of trnsporter configurations related to mRNP export.* Journal of Cell Science, 1998. **111**: p. 223-236.
3. Longest, P.W. and C. Kleinstreuer, *Interacting effects of uniform flow, plane shear, and near-wall proximity on the heat and mass transfer of respiratory aerosols.* International Journal of Heat And Mass Transfer, 2004. **47**(22): p. 4745-4759.
4. Karniadakis, G.E. and A. Beskok, *Microflows: Fundamentals and Simulation*. 2002, New York: Springer Verlag.
5. Gad-el-Hak, M., *The MEMS Handbook*. 2002, New York: CRC Press.
6. Koo, J. and C. Kleinstreuer, *Liquid flow in microchannels: experimetnal oberservations and computational analyses of microfluidics effects.* J. Micromech. Microeng., 2003. **13**: p. 568-579.
7. Mala, G.M. and D. Li, *Flow characteristics of water in microtubes.* International Journal of Heat and Fluid Flow, 1999. **20**: p. 142-148.
8. Longest, P.W., C. Kleinstreuer, and J.R. Buchanan, *Efficient computation of micro-particle dynamics including wall effects.* Computers & Fluids, 2004. **33**(4): p. 577-601.
9. Clift, R., J.R. Grace, and M.E. Weber, *Bubbles, Drops, and Particles*. 1978, New York: Academic Press.
10. Crowe, C., M. Sommerfeld, and Y. Tsuji, *Multiphase Flows with Drops and Bubbles*. 1998, Boca Raton: CRC Press.